Konrad-Zuse-Zentrum
für Informationstechnik Berlin

Takustraße 7
D-14195 Berlin-Dahlem
Germany

ALEXANDER FISCHER FRANK CORDES CHRISTOF SCHÜTTE

Hybrid Monte Carlo with Adaptive Temperature in a Mixed-Canonical Ensemble: Efficient Conformational Analysis of RNA

Preprint SC 97-67 (December 1997)

Hybrid Monte Carlo with Adaptive Temperature in a Mixed-Canonical Ensemble: Efficient Conformational Analysis of RNA

Alexander Fischer Frank Cordes Christof Schütte

Abstract

A hybrid Monte Carlo method with adaptive temperature choice is presented, which exactly generates the distribution of a mixed-canonical ensemble composed of two canonical ensembles at low and high temperature. The analysis of resulting Markov chains with the reweighting technique shows an efficient sampling of the canonical distribution at low temperature, whereas the high temperature component facilitates conformational transitions, which allows shorter simulation times.

The algorithm was tested by comparing analytical and numerical results for the small n-butane molecule before simulations were performed for a triribonucleotide. Sampling the complex multi-minima energy landscape of this small RNA segment, we observe enforced crossing of energy barriers.

Introduction

The efficient sampling of phase space for complex biological systems remains to be the specific problem in theoretical biochemistry. This problem can only be solved with Monte Carlo (MC) or molecular dynamics (MD) simulations, if it is possible to overcome energy barriers, which are large compared to the thermal energy. MC algorithms, that are based on local conformational changes of functional groups, can enforce barrier crossing by significant distortions. Unfortunately, large local distortions are often energetically unfavourable and the corresponding MC proposals will be rejected. One way to overcome this problem is to use hybrid Monte Carlo (HMC) techniques [7, 6, 16], which allow to combine global updates in position space with reasonable acceptance rates. Another way is to sample in so-called generalized ensembles [12], where the canonical ensemble is replaced by a probability density, which supports an extended energy range. Higher energy regions will be visited more often and enable conformational changes more easily. In this case the resulting Markov chain has to be reweighted according to the canonical ensemble of interest. For the construction of a generalized ensemble different techniques can be applied [4].

The classical Ferrenberg–Swendsen scheme [8] uses results from a canonical distribution at one temperature to extrapolate to expectation values of another distribution at a different temperature. But a small difference between the temperatures is necessary to receive statistically reliable results. The reweighting method can be extended to mix data from independent runs [9]. More recently, algorithms were proposed, which sample over the whole energy range [12], like the multicanonical algorithm [3], simulations in a 1/k-sampling [13] and simulated tempering [15]. Similar ideas to overcome energy barriers are tested by using Tsallis statistics [2] and in the J–walking method [11].

Another approach is to sample in the canonical ensemble with a modified potential, e.g., umbrella sampling [18], fluctuating-potential methods [14] and other potential smoothing techniques [4]. With these techniques energy barriers can be lowered, but artefacts could be introduced by the deformation of the original potential.

The methods listed above exhibit the following characteristics: Firstly, any of the generalized ensembles has to be adapted to the system of interest either by connecting distribution parameters to the simulation protocol or making a physically motivated initial modification of the energy function. Secondly, nearly all strategies are based on conventional MC methods. Therefore, pecularities of the HMC scheme, like availibility of momenta or the possibility of modifications in the acceptance step, are not considered.

In this paper we present a specific generalized ensemble, which allows to exploit the advantageous features of HMC. In particular, we propose a mixed-canonical ensemble, which uses the momentum information for introducing an adaptive temperature function and allows a statistical reasonable reweighting to canonical ensemble averages. The resulting method is called adaptive temperature HMC (ATHMC). The only characteristic parameter of the new distribution function can be interpretated in terms of the average potential energy of the canonical ensemble and has to be approximated by an initial simulation. ATHMC still satisfies the detailed balance condition and guarantees statistical convergence.

An oligoribonucleotide, a small RNA segment, serves as an interesting model system, because of its structural flexibility. Although the general properties of the proposed algorithm can be tested very easily and fast on small molecules as n-butane, the application to a triribonucleotide should indicate, whether the method can induce conformational transitions in macromolecules with a remarkable number of degrees of freedom.

Method

HMC and generalized ensembles

A large class of molecular systems can be described by a separated Hamiltonian of the form

$$H(x,p) = T(p) + V(x) = \frac{1}{2}p^T M^{-1} p + V(x). \tag{1}$$

T denotes the kinetic, V the potential energy and M the diagonal matrix of the atom masses. If an observable A is a function of the coordinates only, the canonical ensemble average is given by

$$< A >_\varrho = \frac{\int A(x)\, \exp[-\beta\, V(x)]\, dx}{\int \exp[-\beta\, V(x)]\, dx}$$

where

$$\varrho(x) = \frac{\varrho^*(x)}{Z_\varrho} = \frac{\exp[-\beta\, V(x)]\, dx}{\int \exp[-\beta\, V(x)]\, dx}$$

is the corresponding canonical probability density at temperature $\mathcal{T}$ with partition sum Z_ϱ and so-called inverse temperature $\beta = 1/k_B\mathcal{T}$ [1].

A Metropolis MC method can be used to generate Markov chains of configurations $x^{(k)}$ with $k = 1, \dots, n$, from which expectation values $<A>_\varrho$ of observables A can be calculated by

$$<A>_\varrho = \lim_{n\to\infty} \frac{1}{n} \sum_{k=1}^{n} A(x^{(k)}). \tag{2}$$

Using HMC as a special Metropolis MC algorithm with global updates, the momenta serve as the random variable generally, i.e., new momenta p have to be drawn from a given distribution before each MC step. If we draw the momenta from a Gaussian distribution $\propto \exp[-\beta\, T(p)]$ according to (1), and propose new coordinates x' and new momenta p' by integrating the system through phase space with a reversible and volume preserving discretized flow Ψ^τ (e.g., the Verlet discretization [20]), the new coordinates x' are accepted with a probability of

$$\begin{aligned} P_{\text{acc}} &= \min\big(1, \exp[-\beta\,(H(x',p') - H(x,p))]\big) \\ &= \min\left(1, \frac{\varrho^*(x')\, \exp[-\beta\, T(p')]}{\varrho^*(x)\, \exp[-\beta\, T(p)]}\right). \end{aligned}$$

If we want to use the HMC scheme to sample a generalized ensemble $\mu(x) = \mu^*(x)/Z_\mu$, we have to adjust the acceptance probability to

$$P_{\text{acc}} = \min\left(1, \frac{\mu^*(x')\, \exp[-\beta\, T(p')]}{\mu^*(x)\, \exp[-\beta\, T(p)]}\right) \tag{3}$$

in order to satisfy the detailed balance condition. Generally, the inverse temperature β is not given directly by μ, but has to be chosen appropriately. Thermodynamical averages have now to be calculated by the reweighting method. If the Markov chain generated due to (3) is used to calculate the averages of the quantities $\exp[-\beta\, V(x)]/\mu^*(x)$ and $A(x)\exp[-\beta\, V(x)]/\mu^*(x)$, the quotient of these averages results in

$$\begin{aligned} \lim_{n\to\infty} \frac{\frac{1}{n}\sum_{k=1}^{n} A(x^{(k)})\, \frac{\exp[-\beta\, V(x^{(k)})]}{\mu^*(x^{(k)})}}{\frac{1}{n}\sum_{k=1}^{n} \frac{\exp[-\beta\, V(x^{(k)})]}{\mu^*(x^{(k)})}} &= \frac{\int A(x)\, \frac{\exp[-\beta\, V(\mathbf{x})]}{\mu^*(\mathbf{x})} \mu(\mathbf{x})\, d\mathbf{x}}{\int \frac{\exp[-\beta\, V(\mathbf{x})]}{\mu^*(\mathbf{x})} \mu(\mathbf{x})\, d\mathbf{x}} \\ &= \frac{\int A(x)\, \exp[-\beta\, V(x)]\, dx}{\int \exp[-\beta\, V(x)]\, dx} = <A>_\varrho \ . \end{aligned} \tag{4}$$

Thus, the scalar quantities $\exp[-\beta\, V(x^{(k)})]/\mu^*(x^{(k)})$ are reweighting factors applied on the configurations $x^{(k)}$ generated from a generalized distribution μ. In contrast to (2) canonical averages of A have to be calculated according to (4). The relative magnitude of the reweighting factors along the Markov chain indicates the statistical reliability of the reweighting scheme, which can be evaluated with histogram techniques [8].

[1] k_B=Boltzmann's constant

Mixed-canonical ensemble

To achieve an improved sampling of coordinate space, we propose a mixed-canonical ensemble with a weighting factor composed as the arithmetic average of two Boltzmann factors at inverse temperatures β^- and β^+:

$$\mu^*(x) = \frac{1}{2}\left(\exp[-\beta^-(V(x)-c)] + \exp[-\beta^+(V(x)-c)]\right).$$

The principal idea is, to enforce barrier crossing by the high temperature part, whereas the low temperature part is important for the statistical reliability of the reweighting. Let $\mathcal{T}$, $\mathcal{T}^-$ and $\mathcal{T}^+$ denote the corresponding temperatures for β, β^- and β^+. For $\mathcal{T}^- = \mathcal{T}^+$, μ is identical to the canonical ensemble. Moreover, μ converges to the low or high temperature canonical ensemble, if c tends to ∞ or $-\infty$, respectively. Although the shift in the potential energy introduced by c has no influence on a canonical ensemble, it determines an energy level in the mixed-canonical density, at which weighting according to the low or high temperature changes: If $V(\mathbf{x}) - c < 0$, the contribution of β^- will dominate and for $V(\mathbf{x}) - c > 0$ the contribution of β^+. The persistence in a certain temperature state is controlled by the relation of the parameter c to the potential energy. Because we are interested in expectation values with respect to ϱ, $\mathcal{T}^-$ should be chosen close to $\mathcal{T}$, whereas the $\mathcal{T}^+$ contribution should facilitate energy barrier crossing. Therefore, we can conclude, that the sampling prefers the distribution to $\mathcal{T}^-$, if c will be greater than $< V >_\varrho$. The difference between c and $< V >_\varrho$ determines the amount of sampling at $\mathcal{T}^+$.

HMC with adaptive choice of temperature

For the implementation of the proposed generalized distribution into ATHMC based sampling we have used the following recipe for one update step. Modifications compared to HMC are discussed below. Fixed parameters at the beginning of the procedure are the temperature of interest, the minimal and the maximal temperature of the generalized distribution.

1. *Initialization of momenta p at the inverse temperature $\beta(x)$, which is assumed to be known from the previous step, i.e.,*

$$p \propto \exp\left[-\beta(x)\sum_{j=1}^{s}\frac{p_j^2}{2m_j}\right].$$

2. *Calculation of new coordinates and momenta $(x', p') = (\Psi^\tau)^n\,(x, p)$.*

3. *Computation of $\beta(x')$ due to (6).*

4. *Acceptance of new coordinates x' with a probability*

$$P_{\text{acc}} = \min\left(1, \frac{\mu^*(x')\ \exp[-\beta(x')\,T(p')]}{\mu^*(x)\ \exp[-\beta(x)\,T(p)]}\ \left(\frac{\beta(x)}{\beta(x')}\right)^{s/2}\right), \qquad (5)$$

   otherwise stay in old coordinates x; s denotes the number of degrees of freedom.

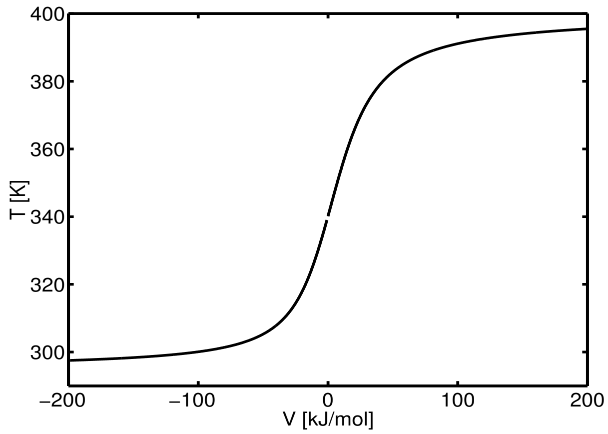

Figure 1: Choice of temperature $\mathcal{T}(x)$ in dependence of the potential energy with $\mathcal{T}^- = 295$ K, $\mathcal{T}^+ = 400$ K and $c = 0$. Note, that the temperature function is directly connected to μ^* and reflects the density of the mixed-canonical ensemble. A change of c induces a change in the density of μ and a shift of the temperature function.

In contrast to (3), the acceptance probability in (5) is once more generalized exploiting the special structure of the mixed-canonical ensemble and taking advantage of the fact, that detailed balance is satisfied for any arbitrary temperature. Instead of using a constant temperature at each step, we search for a temperature function $\beta = \beta(x)$, which depends on the actual potential energy in such a way, that the Boltzmann factor at $\beta(x)$ is equal to $\mu^*(x)$. This results in the temperature function (Fig. 1) [2]

$$\beta(x) = -\frac{\ln \mu^*(x)}{V(x) - c}. \tag{6}$$

With this choice of temperature we can sample from μ in a way which reflects the "local" behavior of the density: Starting a trajectory at x with momenta drawn from a Gaussian distribution corresponding to $\beta(x)$ and arriving at a configuration x' with $\Delta\beta = \beta(x') - \beta(x) \approx 0$, results in an acceptance rate as typically achieved in HMC. Especially, the sampling in low energy regions is dominated by the Boltzmann factor corresponding to β^- with $\beta(x) \approx \beta^-$ and vice versa in high energy regions with $\beta(x) \approx \beta^+$. In these cases, $\Delta\beta$ is low, even if larger changes in the potential energy occur. For other values of $\Delta\beta$ the potential and momenta part of the acceptance step (5) fit together and result also in a reasonable acceptance rate. Therefore, we can expect an acceptance rate close to the corresponding one in a HMC scheme.

Another modification of the acceptance probability (5) comes along with the adaptive temperature. The additional factor $(\beta(x)/\beta(x'))^{s/2}$ in (5) results from the normalization of the two different momentum distributions for $\beta(x)$ and $\beta(x')$, which differ in their standard deviation. Because β remains fixed in HMC, this factor simplifies to 1, see e.g.(3).

[2] For states x with $V(x) = c$ the temperature $\beta(x)$ has to be evaluated by interpolation

The temperature function and the mixed canonical ensemble are simultaneously influenced by the parameter c. Let us assume that c is somewhat larger than the average potential energy with respect to ϱ. Then, the density of the generalized ensemble will enclose the canonical one, but also covers higher energy regions, which has no significance in ϱ. In our case this means, that whenever the potential energy increases in the vicinity of c, kinetic energy is pumped into the system according to the choice of higher temperature for the generation of momenta. Additionally, proposals with higher energy are accepted more easily in μ and the system can move towards higher energy regions, where conformational changes happen more often. Conversely, the system can move from high to low energy regions and eventually arrive in another conformation. Therefore, the fluctuations of $\beta(x)$ serve as a good indicator for the desired behavior and can be used in preliminary runs to find a suitable value for c.

Model systems

The proposed method was tested on two model systems. The n-butane molecule is a very small organic compound. The linear chain consists of four carbons and ten hydrogens. The configuration of the heavy atoms can be described by one torsion angle, two bond angles and three bonds. Significant conformational changes are especially effected by torsion angle rotations. The semiemperical Hamiltonian, which is conventionally used to mimic covalent and non-covalent energy contributions of this kind of macromolecules consists of terms for the kinetic energy, and in its simplest form for bond- and angle oscillations, and torsion angle rotations:

$$\begin{aligned} H(\mathbf{q},\mathbf{p}) &= \frac{1}{2}\mathbf{p}^T M^{-1}\mathbf{p} \\ &+ \sum_{bonds} V_{bonds} + \sum_{angles} V_{angles} + \sum_{torsions} V_{torsions} \\ &+ \sum_{atompairs} (V_{Lennard-Jones} + V_{Coulomb}) \end{aligned}$$

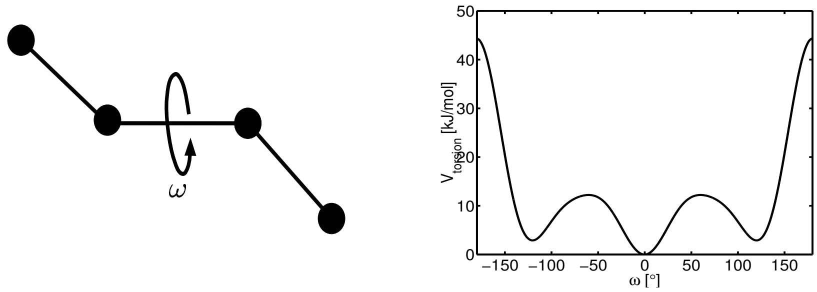

Figure 2: Left: Extended atom model of n-butane with the torsion angle ω. Right: Torsion angle potential. The main minimum corresponds to the *trans* orientation of the angle, the two side minima to the $\pm$*gauche* orientations.

For n-butane we have used the extended atom model of Ryckaert and Bellemans [17] (Fig. 2), which reduces the representation of the chain to the carbon atoms. Moreover, the so-called non-bonded Lennard-Jones and Coulomb interactions play no role for n-butane, because interactions up to the third neighbors are totally covered by the covalent terms. The n-butane molecule with its one torsion angle ω serves as an ideal test system for the proposed ATHMC scheme. Firstly, the three orientations of ω describe also the three possible conformations (see Fig. 2). Secondly, as was shown in [10], the expectation value for the torsion angle potential V_{torsion} can be computed analytically. Therefore, we can compare our results with analytically exact values.

The physical representation of the triribonucleotide (Fig. 3) adenylyl *(3'-5')*cytidylyl*(3'-5')*cytidin [*r(ACC)*] is based on the GROMOS96 extended atom force field [19]. Comparable to the n-alkane model, some non-polar hydrogens are covered by the corresponding heavy atoms. Moreover, GROMOS96 contains an extra covalent energy term for out-of-plane oscillations. The global structure of *r(ACC)* can be roughly described by eight parameters per nucleotide (Fig. 3). The torsion angles χ around the glycosyl bond and the puckering of the ribose ring described by the pseudorotation angle P and its phase θ [1] are of special interest for the conformational analysis.

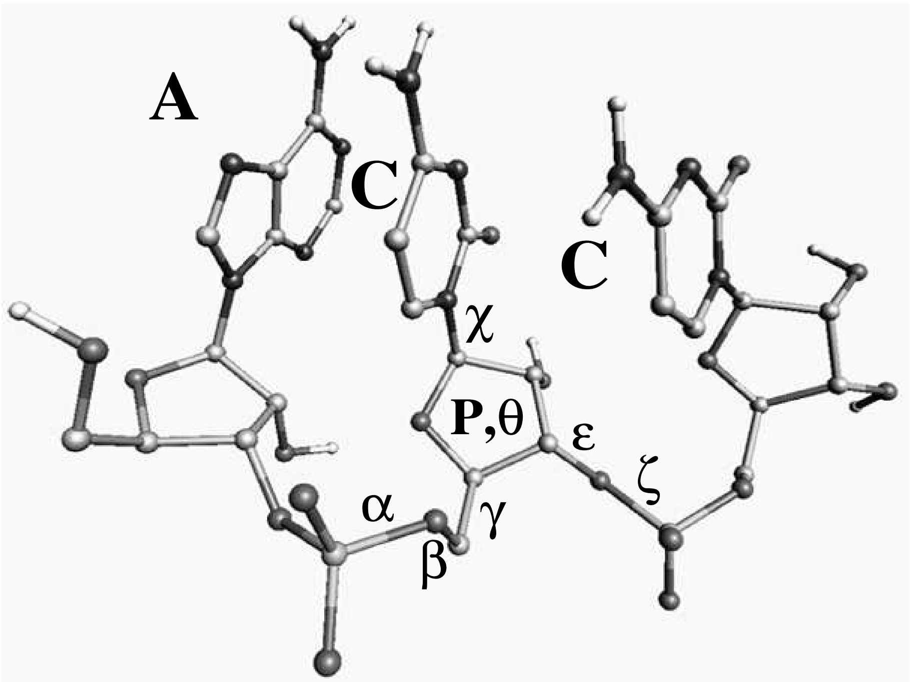

Figure 3: The triribonucleotide adenylyl*(3'-5')*cytidylyl*(3'-5')*cytidin [*r(ACC)*] in the extended atom representation of GROMOS96 [19]. A and C denote the bases adenine and cytosine. Small greek letters refer to the set of torsion angles, which is necessary for a rough reconstruction of the molecule's configuration. The torsion angles of the ribose can be approximated by the pseudorotation angle P and the phase θ [1].

Results and Discussion

The n-butane molecule

For simulations of n-butane, we used the Verlet scheme [20] with $n = 40$ iterations and a time step of $\tau = 15\,\text{fs}$, which results in a trajectory length of $600\,\text{fs}$ for each update step. Performing a simulation over 10^5 steps at a temperature of $\mathcal{T} = 100\,\text{K}$ with HMC (not shown here), we observed a trapping of the Markov chain in the +gauche conformation, where we started the simulation. The energy barrier towards the trans conformation seems to be too high at this low temperature to be overcome in a reasonable simulation time.

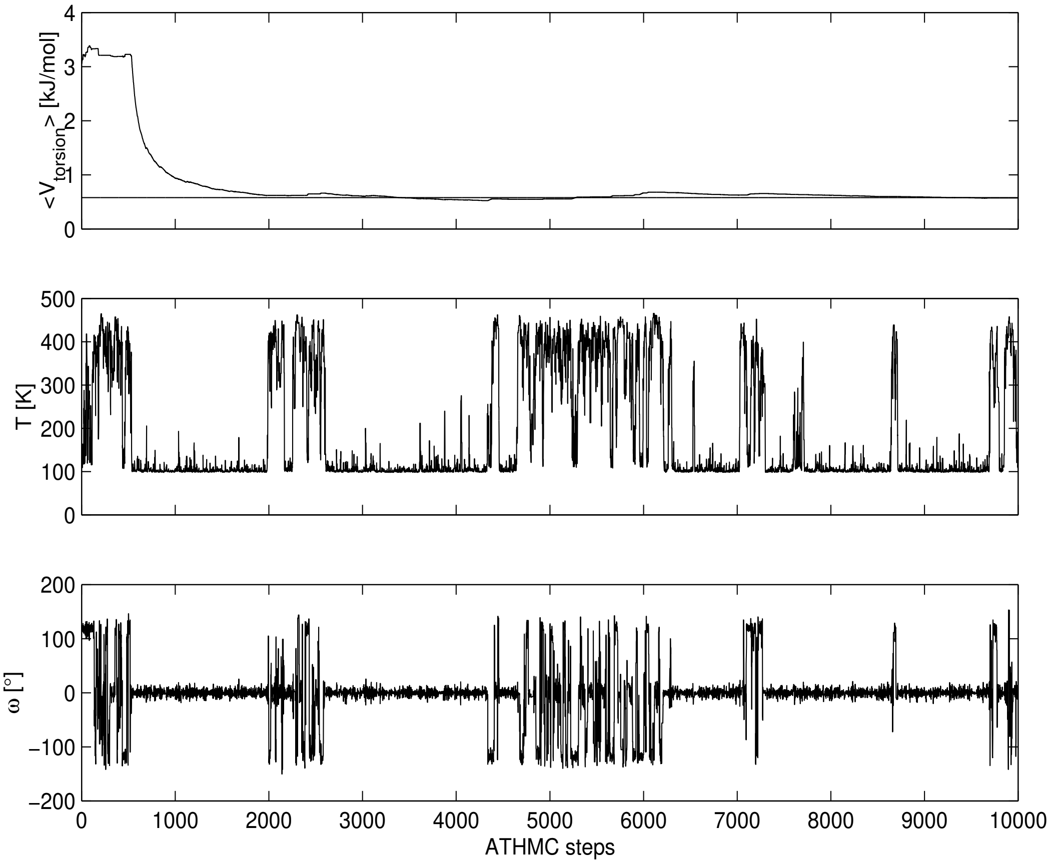

Figure 4: ATHMC run for n-butane. The simulation was performed for 10^4 steps with $\mathcal{T} = 100\,\text{K}$, $\mathcal{T}^- = 90\,\text{K}$, $\mathcal{T}^+ = 500\,\text{K}$ and $c = 1.5$. The flat line in the first subplot indicates the analytically computed expectation value.

Sampling the position space with ATHMC with only 10^4 steps (Fig. 4) and carrying out the reweighting (4) to the temperature of interest at $\mathcal{T} = 100\,\text{K}$, leads us to a distribution of the three conformations of ω and to an expectation value of $< \mathrm{V}_{\mathrm{torsion}} >$ close to the analytic values:

	$<\mathrm{V}_{\mathrm{torsion}}>$	$-$gauche in %	trans in %	$+$gauche in %
analytic values	0.571	2.40	95.20	2.40
HMC	3.353	0	0	100
ATHMC (reweighted)	0.580	3.15	94.24	2.61

The simulations on n-butane in μ were easily adapted to a suitable parameter set by short preliminary runs without the need of fine tuning. The acceptance rate decreased only slightly from 83.1% to 75.3% by changing from HMC to the ATHMC scheme.

Figure 4 illustrates, that a change of the torsion angle orientation is directly correlated to the choice of temperature. We can observe the behavior as described in the previous section. Note, that most of the time the Markov chain samples at $\mathcal{T} \approx \mathcal{T}^-$, which guarantees the statistical reliability of the reweighting.

The triribonucleotide *r(ACC)*

HMC simulations on *r(ACC)* were performed over $5 * 10^5$ steps. The discretized flow was again realized by the Verlet integrator [20] with a time step of $\tau = 2\,\mathrm{fs}$ over $n = 40$ iterations between two HMC updates. Compared to n-butane, a much smaller time step and MD-trajectory is required to guarantee an acceptance rate of 58.7%. The c parameter for the ATHMC calculations was first adjusted to an approximated averaged potential energy, which results from preliminary short HMC cycles. In subsequent short test calculations c was then slowly shifted towards higher energies. The preprocessing was finished at a total shift of 50 kJ/mol. At this point a temperature fluctuation between $\mathcal{T}^- = 295\,\mathrm{K}$ and $\mathcal{T}^+ = 400\,\mathrm{K}$ is reached, which basically prefers the low temperature (Fig. 5). The adjustment of c depends strongly on the difference between the two temperatures and the expected energy fluctuations of the simulation. The butane molecule with only a few degrees of freedom allows larger jumps in temperature or kinetic energy, respectively. It appears, that the ATHMC finds pathways from low to high energy regions. Test calculations for the triribonucleotide on the other hand show, that at $\mathcal{T}^+ = 500\,\mathrm{K}$, *r(ACC)* could be brought into a high energy state during the simulation, but will not relax again. Large temperature differences will narrow the range around c, in which a moderate transition between the two corresponding energy regions can take place.

The development of the averaged potential energy in ATHMC (Fig. 5) and HMC (Fig. 6) demonstrates the superiority of the adaptive temperature choice in the mixed-canonical ensemble. The averaged energy converges faster to a slightly lower value. Although the temperature difference of 105 K is smaller than in the n-butane case and the global updates are based on shorter MD simulations, Fig. 6 illustrates the ability of the method to induce global conformational changes. This behavior should be examined on some selected parameters of the cytidylyl group. The torsion angle around the glycosyl bond χ mainly oscillates in the range between -160° and -80°, but is shifted at least four times towards the range between 40° and 100°. Even more conformational transitions can be observed in the backbone for the torsion angle γ.

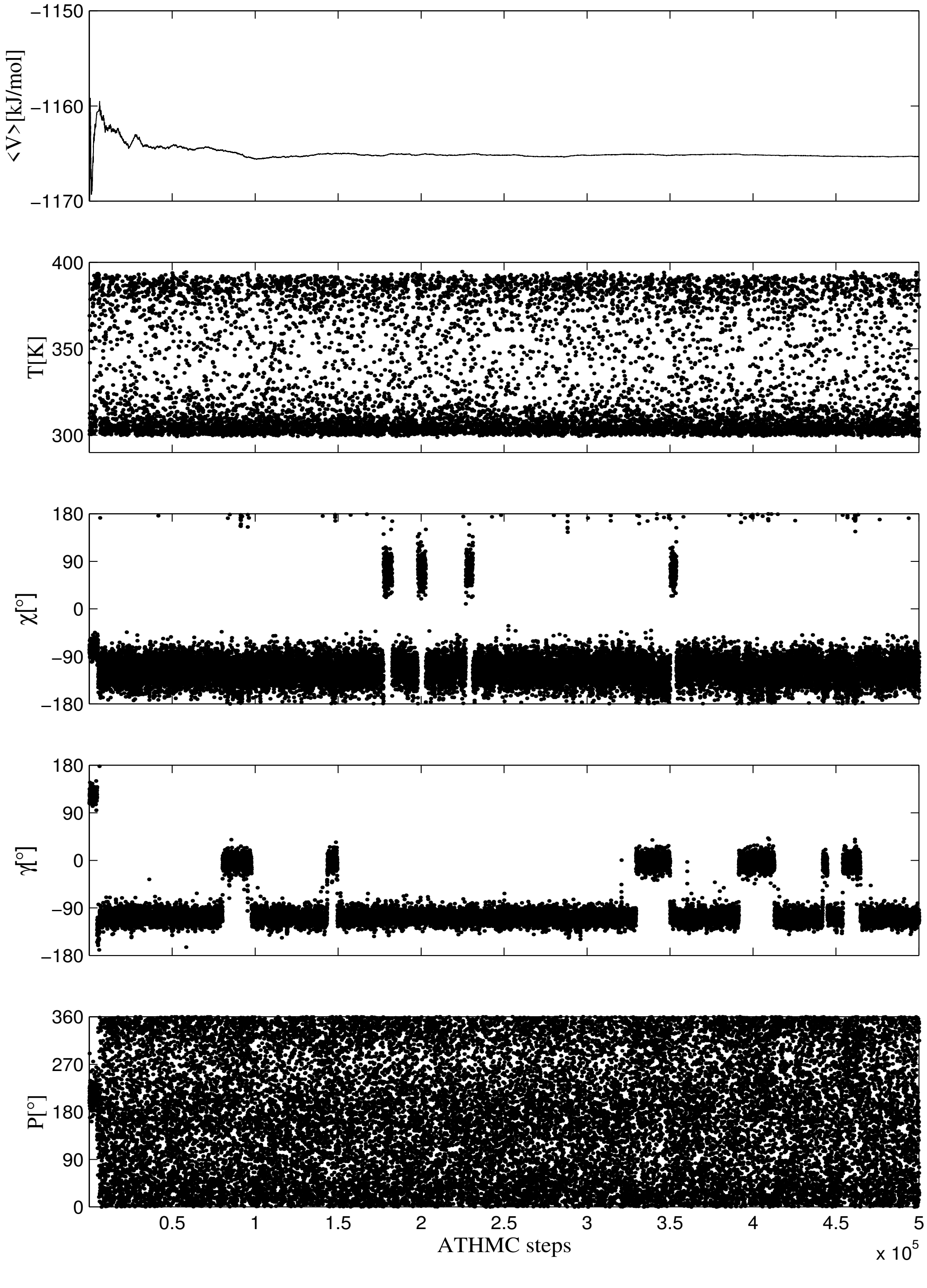

Figure 5: ATHMC run for *r(ACC)*. The simulation was performed for $\mathcal{T}^- = 295\,\mathrm{K}$, $\mathcal{T}^+ = 400\,\mathrm{K}$ and $c = -1121.$ kJ/mol. The averaged potential energy $< V >$, the temperature $\mathcal{T}$, and for the cytidylyl group the torsion angles χ and γ and the pseudorotation angle P are displayed at every twentieth step.

The backbone transitions are clearly uncoupled from the glycosyl transitions, but highly correlated to the dynamics of the other internal coordinates of the backbone, β, ϵ and ζ (not shown here). In our simulations the torsion angle α shows no distinguishable transitions, whereas the pseudorotation angle P is spread over its whole definition range.

These results of ATHMC are in contrast to normal HMC, which should be discussed on γ and P (Fig. 6). In HMC γ remains almost in the initial state. The only exception at the beginning between 50000 and 80000 steps probably results from the equilibration of the system, which is not finished at this stage. Additionally, the ribose ring described by the pseudorotation angle P and the phase θ clearly occupies only one preferred conformation. The averaged potential energy converges very slow and stays slightly above the value of ATHMC. Again HMC is not able to enforce the necessary conformational changes, which bring the system into more preferable conformations. Moreover, Fig. 5 and Fig. 6 demonstrates, that ribose puckering is very sensible to the temperature.

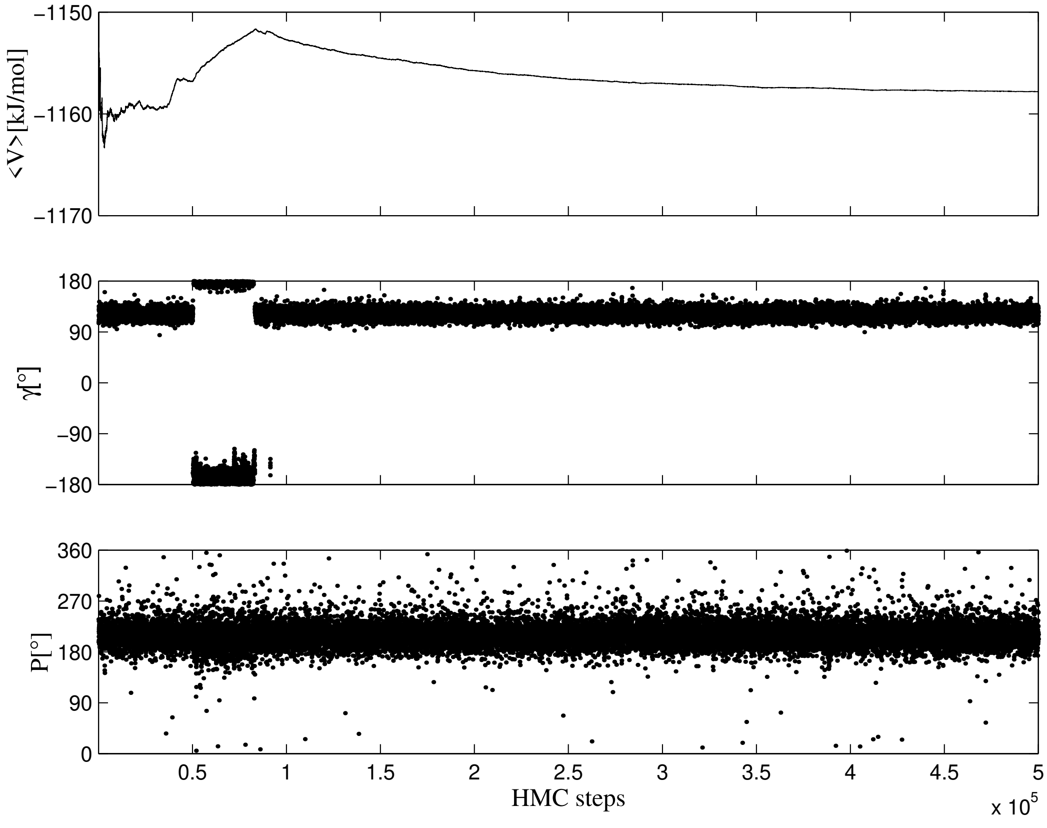

Figure 6: HMC for *r(ACC)* in the canonical ensemble. The simulation was performed for $\mathcal{T} = 300$ K. The averaged potential energy $< V >$ and for the cytidylyl group the torsion angle γ and the pseudorotation angle P are displayed at every twentieth step.

To investigate the dependence between the temperature choice and conformational transitions in more detail, we now zoom to the first 10000 steps of the ATHMC run (Fig. 7). The averaged potential energy in Fig. 5 and 6 indicate, that the arbitrarily chosen initial conformation of the simulation belongs to an energy below the average, which makes a transition to another more realistic conformation desirable. The γ torsion at this starting point is around $120°$. Normal HMC (Fig. 6) is unable to induce a necessary transition to another state. Only the heating of the system due to the choice of momenta according to higher temperature induces the necessary transition of γ around step 4500.

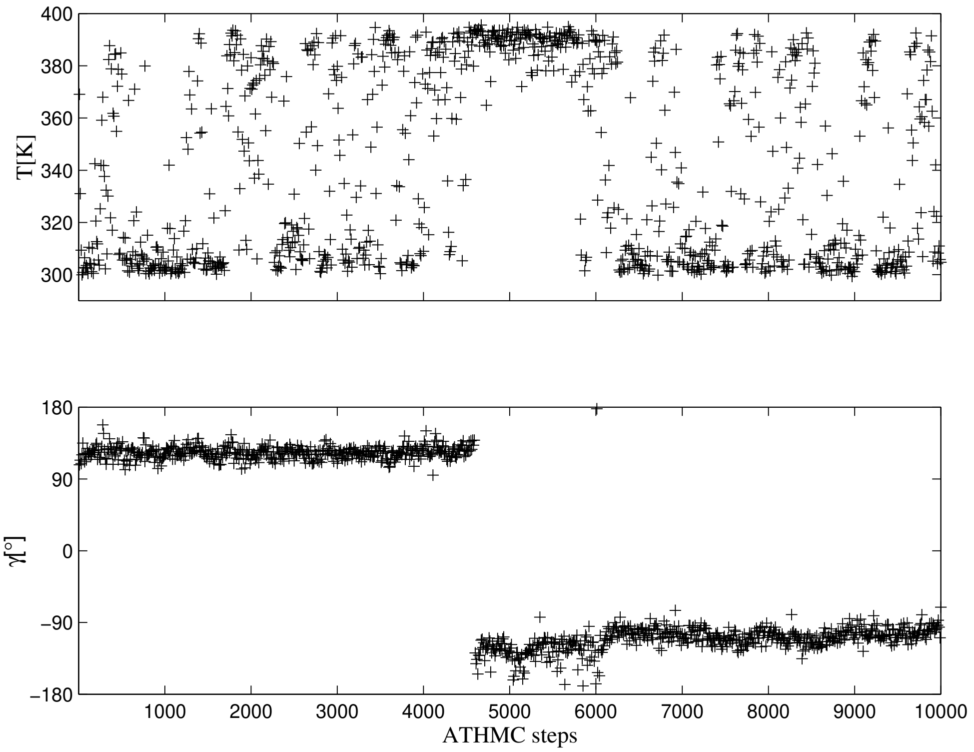

Figure 7: ATHMC for *r(ACC)* in the mixed-canonical ensemble. The simulation was performed for $\mathcal{T}^- = 295\,\mathrm{K}$, $\mathcal{T}^+ = 400\,\mathrm{K}$ and $c = -1121\,\mathrm{kJ/mol}$. The temperature $\mathcal{T}$, and for the cytidylyl group the torsion angle γ are displayed at every tenth step over the first 10000 steps.

The fact, that ATHMC samples at different temperatures with sufficient rates, is furthermore illustrated by the probability distribution of energy before and after the reweighting (Fig. 8). Without reweighting (equation 4) we observe a maximum around the averaged potential energy, but another distribution peak for higher energies, exactly enforced by the choice of higher temperatures and the non-negligible acceptance at higher energies. Fig. 8 makes the strategy of generalized ensembles very clear, that is to overcome energy barriers by sampling not only low but also high energy areas. The idea of equalizing the energy distribution over an extended energy range finds its extreme realization in the multi-canonical approach [12], which is orientated on a constant distribution. ATHMC also stretches the energy distribution, but is conceptionally still connected to the physical properties of the system, indicated by the great overlap of canonical and mixed-canonical distribution.

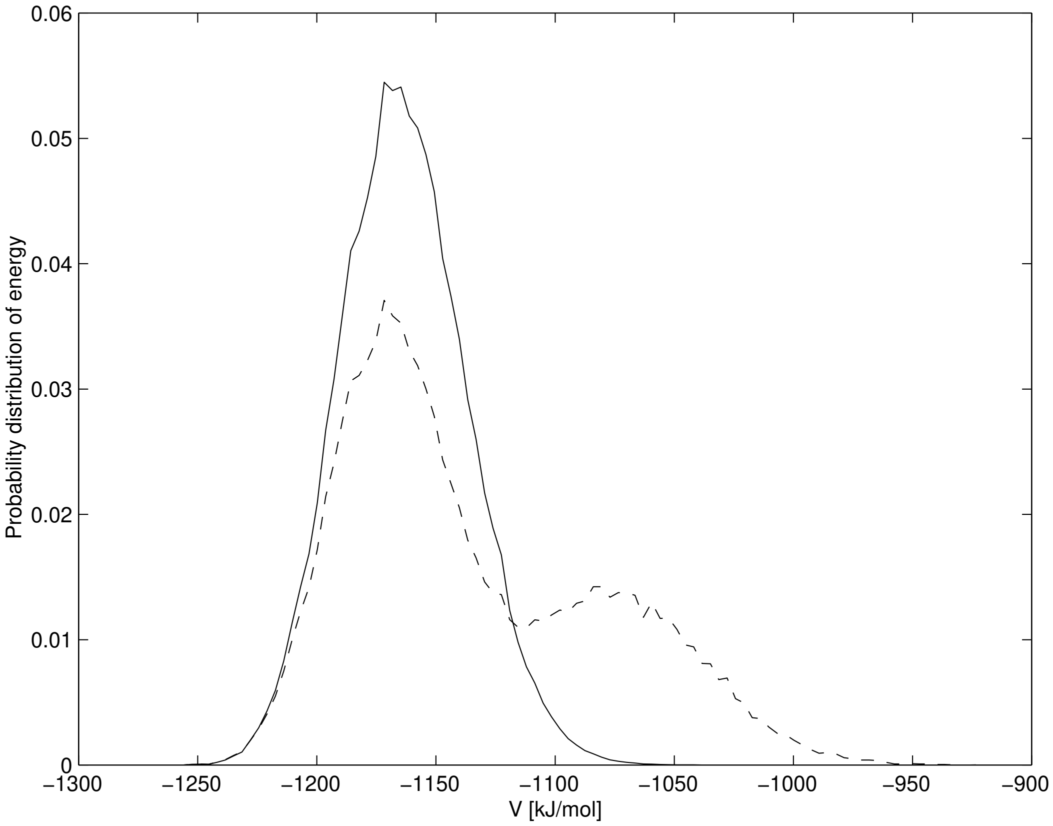

Figure 8: ATHMC for *r(ACC)* in the mixed-canonical ensemble. Probability distribution of energy before (dashed line) and after (solid line) reweighting. Computed according to equation (4).

Conclusion

The ATHMC method presented herein permits to realize an adaptive temperature choice in a generalized ensemble. The crucial detailed balance condition remains to be valid in ATHMC, because the separation of coordinates and momenta in the acceptance step is possible.

The comparision of conventional HMC and ATHMC exhibits the superiority of the latter with respect to the conformational analysis of biomolecules. The adaptive temperature choice coupled with a generalized, mixed-canonical ensemble was discussed to be responsible for the efficient sampling properties. Like all other strategies based on generalized ensembles the proposed algorithm cannot relinquish pre- and postprocessing procedures. But preprocessing in ATHMC needs only one parameter, c, which corresponds to the averaged potential energy of the system. The simplicity of this approach may be advantegeous for applications to larger molecules, because even an insufficient determination of c will give reliable statistical results: If c deviates too much from its optimal value one of the canonical distributions will dominate the sampling. Moreover, the influence of c on the temperature fluctuations can even control the equilibration state of the system.

In a forthcoming work it will be of special interest to include the solvent environment into ATHMC in order to investigate its influence on temperature choice, determination of c and acceptance rate. Again oligoribonucleotides can serve as a good model system, because the availibility of theoretical as well as experimental data from NMR measurements [5] makes quantitative predictions possible.

References

[1] C. Altona and M. Sundaralingam. Conformational analysis of the sugar ring in nucleosides and nucleotides. a new description using the concept of pseudorotation. *JACS*, 94:8205–8212, 1972.

[2] I. Andricioaei and J.E. Straub. Generalized simulated annealing algorithms using Tsallis statistics: application to conformational optimization of a tetrapeptide. *Phys. Rev. E*, 53:3055–3058, 1996.

[3] B.A. Berg and T. Neuhaus. Multicanonical algorithms for first order phase transitions. *Phys. Lett. B*, 267:249–253, 1991.

[4] B.J. Berne and J.E. Straub. Novel methods of sampling phase space in the simulation of biological systems. *Curr. Opinion Struct. Biol.*, 7:181–189, 1997.

[5] N. Bouchemal-Chibani, C.Herve du Penhoat, M. Abdelkafi, M. Ghomi, and P.Y. Turpin. Characterization of the dynamic behavior of r(ACC) and r(AAC) with NMR relaxation data and both Metropolis Monte Carlo and Molecular Dynamics simulations. *Biopolymers*, 39:549–571, 1996.

[6] A. Brass, B.J. Pendleton, Y. Chen, and B. Robson. Hybrid Monte Carlo simulations theory and initial comparison with molecular dynamics. *Biopolymers*, 33:1307–1315, 1993.

[7] S. Duane, A.D. Kennedy, B.J. Pendleton, and D. Roweth. Hybrid Monte Carlo. *Phys. Letters B*, 195(2):216–222, 1987.

[8] A.M. Ferrenberg and R.H. Swendsen. New Monte Carlo technique for studying phase transitions. *Phys. Rev. Letters*, 61(23):2635–2638, 1988.

[9] A.M. Ferrenberg and R.H. Swendsen. Optimized Monte Carlo data analysis. *Phys. Rev. Letters*, 63(12):1195–1197, 1989.

[10] A. Fischer. Die Hybride Monte–Carlo Methode in der Molekülphysik. Diploma thesis, Freie Universität Berlin, 1997.

[11] D.D. Frantz, D.L. Freeman, and J.D. Doll. Reducing quasi-ergodic behavior in Monte Carlo simulation by J-walking: applications to atomic clusters. *J. Chem. Phys.*, 93:2769–2784, 1990.

[12] U.H.E. Hansmann and Y. Okamoto. Numerical comparison of three recently proposed algorithms in the protein folding problem. *J. Comput. Chem.*, 18:920–933, 1997.

[13] B. Hesselbo and R.B. Stinchcombe. Monte Carlo simulation and global optimization without parameters. *Phys. Rev. Lett.*, 74:2151–2155, 1995.

[14] Z. Liu and B.J. Berne. Methods for accelerating chain folding and mixing. *J. Chem. Phys.*, 99:6071–6077, 1993.

[15] E. Marinari and G. Parisi. Simulated tempering: a new Monte Carlo scheme. *Europhys. Lett.*, 19:451–458, 1992.

[16] B. Mehlig, D.W. Heermann, and B.M. Forrest. Hybrid Monte Carlo method for condensed-matter systems. *Phys. Rev. B*, 45(2):679–685, 1992.

[17] J.-P. Ryckaert and A. Bellemans. Molecular dynamics of liquid alkanes. *Faraday Discuss.*, 66:95–106, 1978.

[18] G.M. Torrie and J.P. Valleau. Nonphysical sampling distributions in Monte Carlo free-energy estimation: Umbrella sampling. *J. Comput. Phys.*, 23:187–199, 1977.

[19] W.F. van Gunsteren, S.R Billeter, A.A. Eising, P.H. Hünenberger, P. Krüger, A.E. Mark, W.R.P. Scott, and I.G. Tironi. *Biomolecular Simulation: The GROMOS96 Manual and User Guide*. vdf Hochschulverlag AG an der ETH Zürich, 1996.

[20] L. Verlet. Computer “experiments” on classical fluids. I. Thermodynamical properties of Lennard-Jones molecules. *Phys. Rev.*, 159:98–103, 1967.